

Methodology and results of Nile Delta Messinian-Pliocene Holistic 3D seismic interpretation

A case study from the Disouq area, Onshore Nile Delta, Egypt

Tarek S. Ellaihy¹, Alexander Prexl¹, Nicolas Daynac²

(1) DEA Egypt Branches, (2) Eliis SAS, France

Introduction

During the last decade DEA Egypt made several gas discoveries in Messinian and Pliocene sandstone reservoirs in the Nile Delta Basin. In the Disouq fields DEA is producing from the Messinian reservoirs while the Pliocene succession is considered to be only little prospective. Small HC accumulations in the Pliocene might however be incorporated at later stages.

In 2013/2014 DEA performed a new data merge and re-processing of the available 3D seismic data covering the Disouq DLA. The improved seismic image led to a better understanding particularly of the Messinian-Pliocene sedimentation.

Traditionally 3D seismic interpretation is performed on 2D sections and subsequently 3dimensional refined using auto-tracking methods. This process is time consuming and hence limited to a low number of interpreted horizons. Under time constraints this can cause important details to be overseen.

Beside of conventional 3D interpretation a holistic geo-modelling approach was carried out in order to create a detailed model of all potential reservoir intervals. Also this workflow was intended as a feasibility study for a fast detailed 3D seismic interpretation in the Delta.

Global approaches have been proposed to compute Relative Geological Time (RGT) models directly from the seismic data without the need to pick all horizons manually (Pauget et al., 2009). In this study a 3D Geomodel software was used, which is based on the Global Optimization Method (Hoyes & Cheret, 2011). Initially a 3D model was computed using the minimization of a cost function, which depends on the distance and the similarity of the mini-traces between seismic points. This process automatically tracks all inflection points within the seismic volume to constrain a grid where a relative geological time is computed for every point. The interpreter afterwards checked relationships between horizons and refined the links between the nodes inside the grid until an optimum solution was obtained.

This technique allowed the creation of both a high resolution geomodel and an almost infinite number of chronostratigraphic horizons. Based on the latter geobody detection, attribute extraction as well as a fast spectral decomposition was performed and wheeler diagrams were composed on the fly. The advantages and limitations of the method will be explained and intermediate results presented.

Methodology

The method to obtain a Relative Geological Time (RGT) model from the seismic is a three-step workflow. During a first step, a grid is computed, where nodes are created vertically at every peak, trough and/or other inflection point. Each node represents the center of an elementary horizon patch with a constant size. The patch size is defined by the spatial resolution of the model grid (s. fig-1). In the second step the algorithm automatically tracks every horizon within the seismic volume to constrain the grid and to connect the individual patches to relative geological time surfaces. During a third step, the relationships between horizons patches are manually checked in order to refine the links between the nodes inside the grid until an optimum; geo-sensitive solution is obtained incorporating the knowledge of the different sequences and the geological markers.

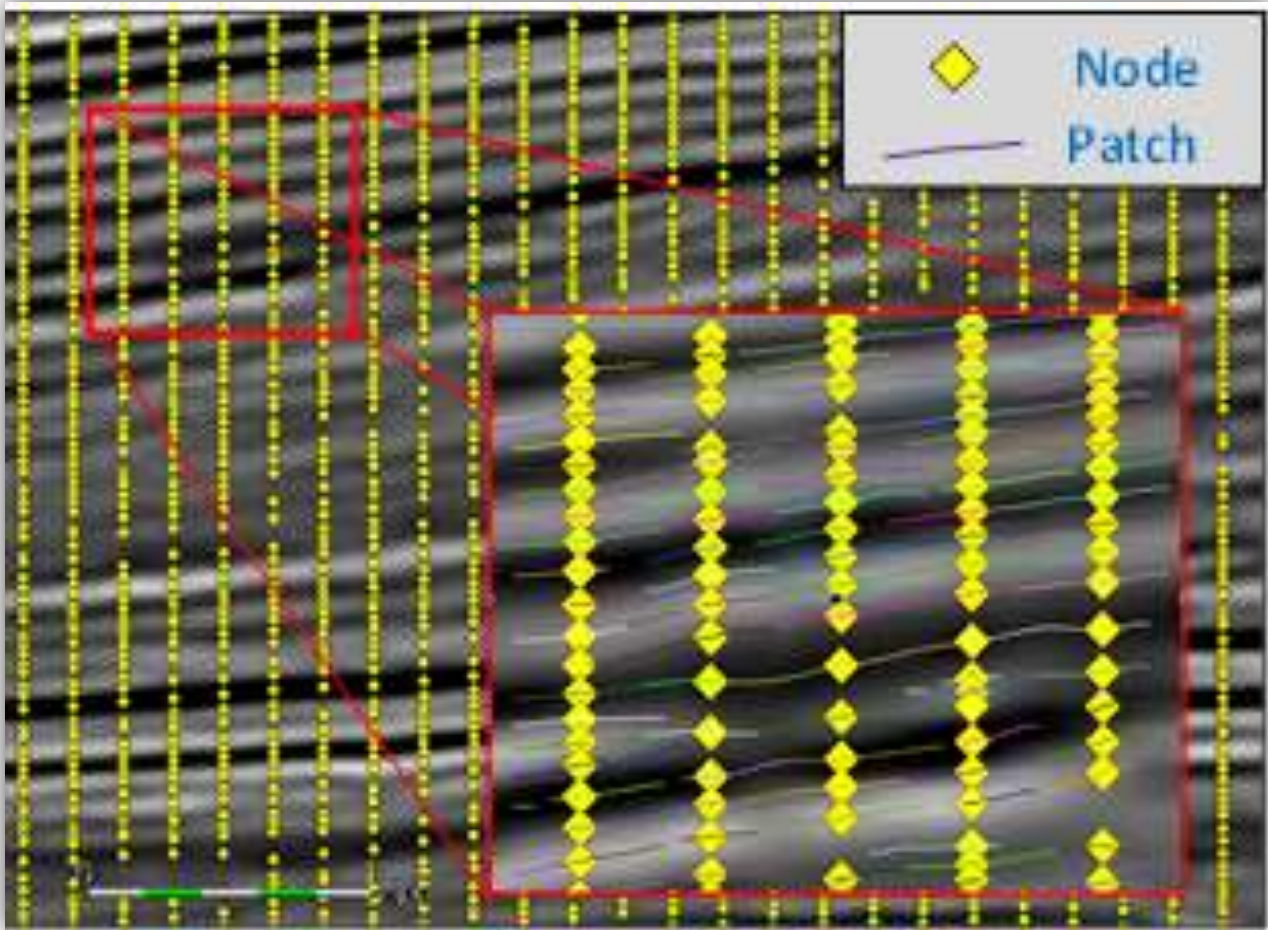


Fig. 1: The number of nodes in the Model Grid is limited. This number will depend on the size of the patches respectively trace increment. The smaller the trace increment, the smaller is the size of the individual patches and the higher is their total number (and vice versa).

Subsequently a 3D continuous Relative Geological Time (RGT) model was computed between the top & bottom boundaries of the Model-Grid (here Top Pliocene - Base Messinian) based on the last two steps workflow (s. fig-2). Horizons were extracted from the RGT-model covering the full area of the volume. Effectively an unlimited number of horizons become available which can be scrolled through like through the time-slices of a seismic volume but following the interpreted stratigraphic layers.

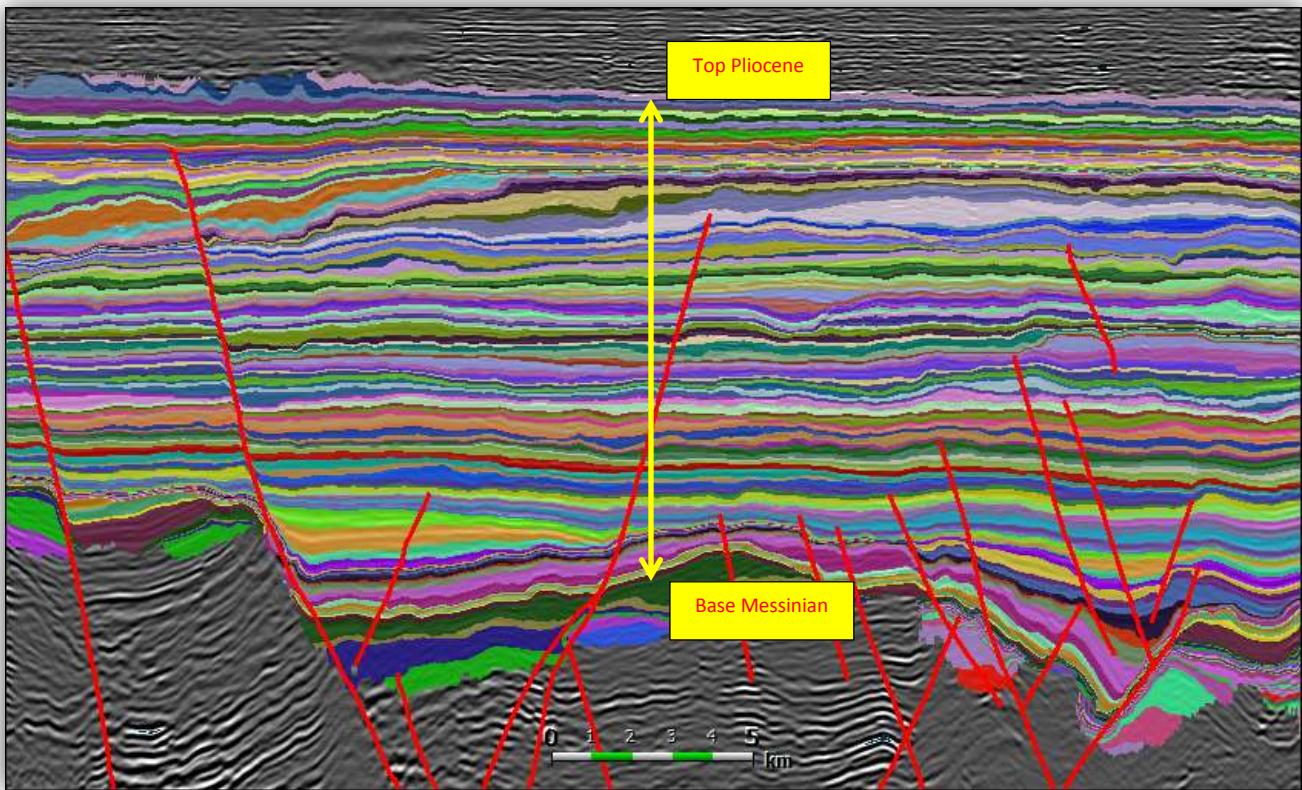


Fig. 2: Relative Geological Time (RGT) model computed between top & bottom boundaries of the Model-Grid (Top Pliocene - Base Messinian)

A new useful attribute became available by the computation of the vertical derivatives of the RGT model (s. fig-3a, 3b). This so called "*Thickness*" cube reveals the instantaneous thickness variations of the geological layers in the volume on each seismic voxel.

It highlights zones showing the convergence and divergence of the geological layers as unconformities, stratigraphic terminations (downlap, onlaps and toplap), erosions, compaction and basin levels.

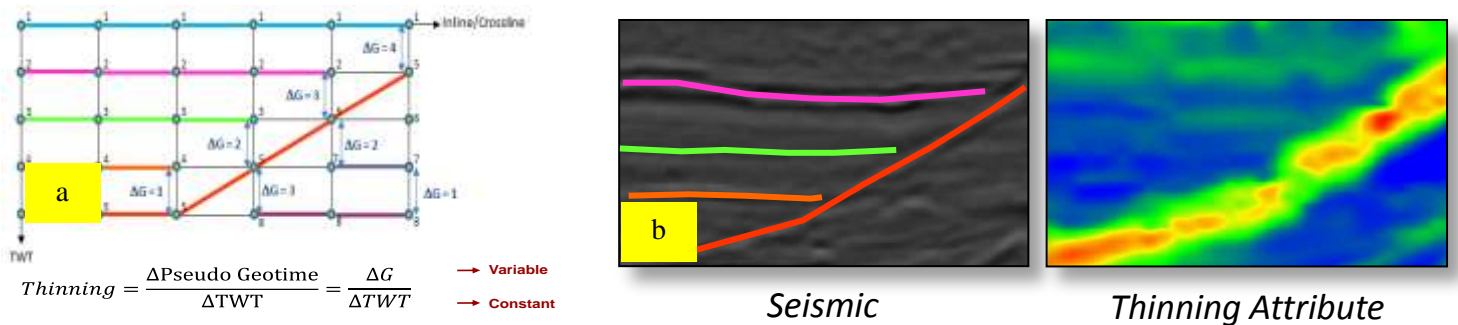


Fig. 3a: Definition of the “thickness” attributes. A value of thickness corresponds to the vertical derivative of the relative geological time model computed for every seismic voxel. Fig. 3b: The thickness attribute enhances stratigraphic discontinuities.

Another outcome of the RGT model is an almost unlimited number of chronostratigraphic consistent horizons used to explore and interpret the geomorphological elements in the volume. This tool enables also an interactive strata slicing through the seismic volume where sedimentary as well as structural features can be highlighted with an unprecedented level of accuracy. Detailed Geobody interpretation on the reprocessed seismic volume enables precise extraction of the geological features constrained by the RGT stratigraphy (s. fig-4a, 4b).

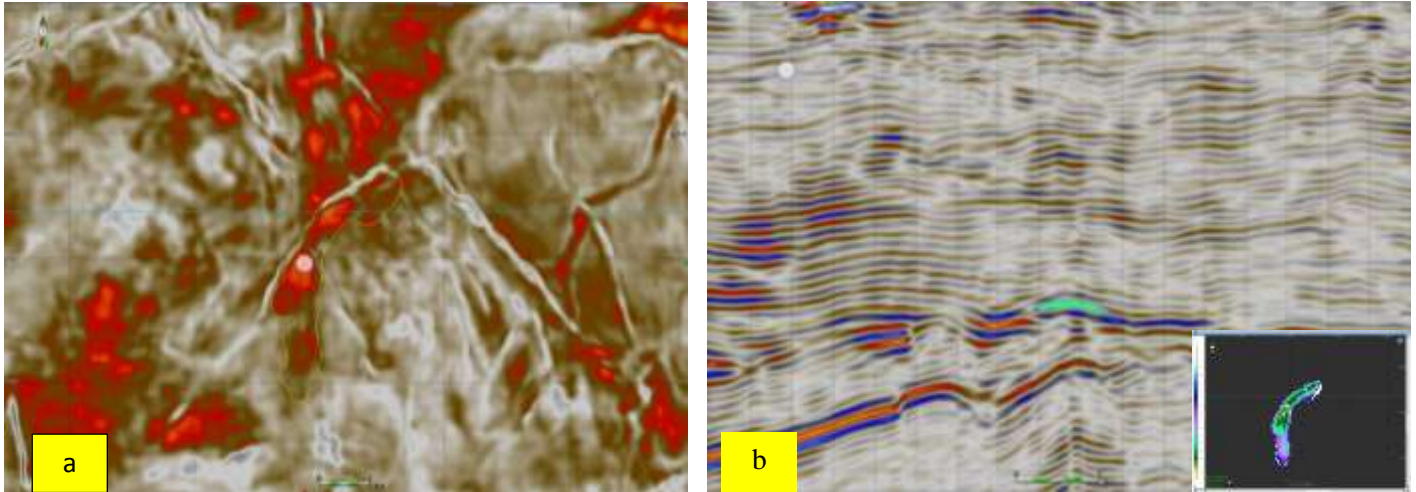


Fig.4a: With a high level of accuracy structure elements and stratigraphic features could be clearly detected using the horizon-stack technique. Fig-4b: Geobody detection and interpretation.

Spectral Decomposition

Spectral Decomposition extracts band limited versions of the data by decomposing the frequency spectrum of the seismic data into three band passes and assigns colour for each band pass (RGB) (Red-Green-Blue) and offers a much more sensitive method of analyzing seismic data than the full frequency amplitude response Fig.5.

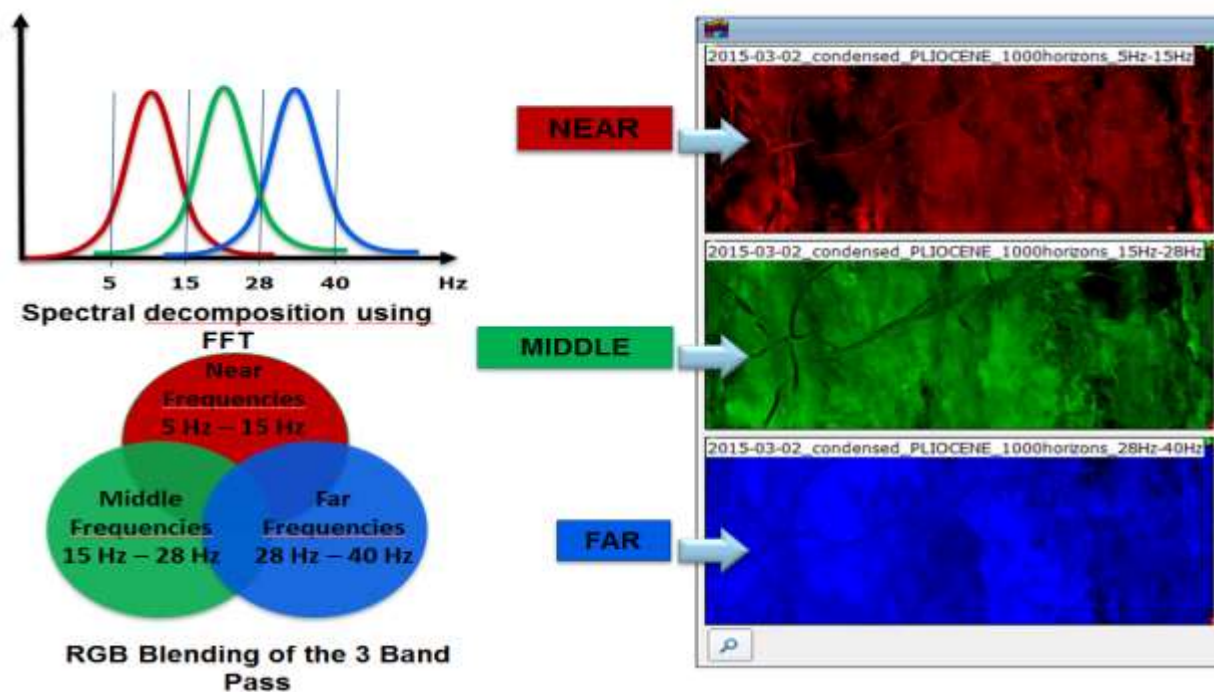


Fig.5a dividing the spectrum of the seismic data into three band pass frequencies (Near frequencies 5 Hz–15 Hz, Middle Frequencies 15 Hz–28 Hz, and Far Frequencies 28 Hz–40Hz).

When 3 frequency magnitude responses are combined in an RGB colour blend, the relationships and interplay between the frequency responses can be investigated. The colour and intensity apparent in the RGB blend depend on a number of variables related to the frequency and amplitude of the signal, Which It can provide information about stratigraphic facies boundaries, structural and stratigraphic geometries Fig. 6a,b.

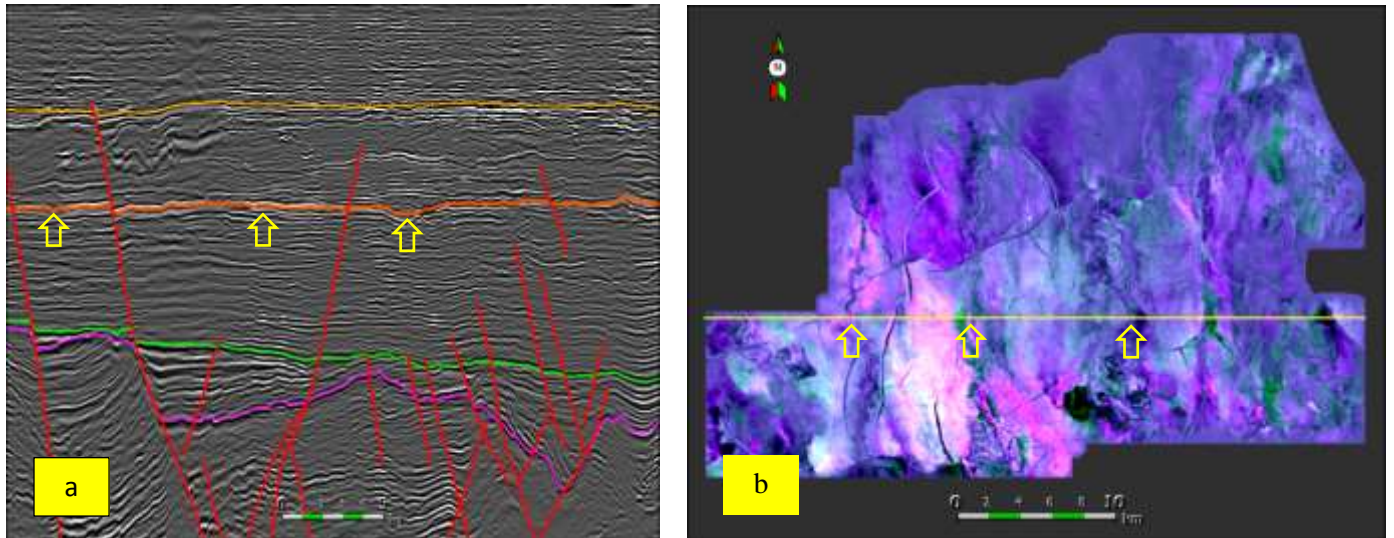


Fig 6a Seismic section across three channels in Pliocene Fig-6b Horizon slice using RGB colour blinding volume showing N-S channel meandering direction clear.

Conclusions

An alternative interpretation workflow based on a full volume seismic interpretation technique was applied and demonstrated through a case study. A derived sequence stratigraphic interpretation was used to establish and refine a model of the depositional environment and formed the framework for the geo-body extraction using different attributes.

This technique is available using specialised but “of-the-shelf” software and has proven to be a very effective and accurate technique, which is well applicable in the Nile Delta where data quality is sufficient and structural complexity limited.

Acknowledgement

We would like to thank DEA Egypt Branches and Eliis SAS, France for their review and kind permission to publish this article. The work presented in this study is part of DEA’s exploration activities in Egypt.

References

- Hoyes, J. & Cheret, T. (2011). A review of “global” interpretation methods for automated 3D horizon picking. *The Leading Edge*, 30(1), 38-47
- Pauget, F., Lacaze, S. & Valding, T. (2009). A global interpretation based on cost function minimization: 79th Annual International Meeting, SEG, Expanded Abstracts, 2592-9